



ELSEVIER

Physica D 89 (1995) 71–82

PHYSICA D

Lyapunov exponents for a Duffing oscillator

Andrea R. Zeni^{a,1}, Jason A.C. Gallas^{a,b,2}^a Instituto de Física, Universidade Federal do Rio Grande do Sul, 91501-970 Porto Alegre, Brazil^b Höchstleistungsrechenzentrum, Forschungszentrum Jülich, D-52425 Jülich, Germany

Received 15 February 1995; accepted 31 May 1995

Communicated by Y. Kuramoto

Abstract

With the help of a parallel computer we perform a systematic computation of Lyapunov exponents for a Duffing oscillator driven externally by a force proportional to $\cos(t)$. In contrast to the familiar situation in discrete-time systems where one finds “windows” of regularity embedded in intervals of chaos, we find the continuous-time Duffing oscillator to contain a quite regular repetition of relatively self-similar “islands of chaos” (i.e. regions characterized by positive exponents) embedded in large “seas of regularity” (negative exponents). We also investigate the effect of driving the oscillator with a Jacobian elliptic function $\text{cn}(t, m)$. For $m = 0$ one has $\text{cn}(t, 0) \equiv \cos(t)$, the usual trigonometric pumping. For $m = 1$ one has $\text{cn}(t, 1) \equiv \text{sech}(t)$, a hyperbolic pumping. When $0 < m < 1$ the Jacobian function is an intermediary double-periodic function with periodicity depending on m and with Fourier spectrum consisting of a regular train of narrow lines with varying envelope. Using m to tune the drive appropriately one may displace the islands of chaos in parameter space. Thus, Jacobian pumping provides a possible way of “cleaning chaos” in regions of the parameter space for periodically driven systems.

1. Introduction

The purpose of this paper is to report a systematic computation of *Lyapunov exponents* [1–4] for a Duffing oscillator driven externally by periodic forces. As is well known, Lyapunov exponents are very interesting quantities to probe dynamical systems in that they provide a quantitative criteria allowing one to discriminate between asymptotically periodic and aperiodic³

behaviors for sets of parameters and/or initial conditions. For example, by computing Lyapunov exponents one may construct phase diagrams showing regions characterized by periodic motions (i.e. by negative exponents) or aperiodic behaviors (positive exponents). In other words, one may use Lyapunov exponents to discriminate regions characterized by chaotic or non-chaotic behaviors.

A major difficulty in employing Lyapunov exponents for producing phase diagrams for dynamical systems defined by differential equations is that an accurate determination of the exponents involves rather time-consuming computations. With the help of a scalable distributed multicomputer we have been able to generate a relatively large number of Lyapunov expo-

¹ E-mail: andrea@ifl.ufrgs.br² E-mail: jason@hlrserv.hlrz.kfa-juelich.de³ Here the terms “chaotic” and “aperiodic” are used as synonyms. The word “aperiodic” seems more appropriate because it represents more faithfully what is actually observed in our numerical experiments: *absence of periodicity* (i.e. absence of non-positive exponents) within the accuracy of the numerical work, which is high.

nents and to use them to investigate the dynamical behavior present in a well-known physical oscillator: a Duffing oscillator. We have performed two numerical experiments for this oscillator, experiments that are reported in this paper. However, before discussing them, since there are many different “Duffing equations” in the literature, it is perhaps appropriate to explain what we mean by “Duffing” equation.

Duffing [5] considered modeling forced oscillations using several different differential equations, aiming at reproducing his observations of the behavior of machines. He was an engineer interested in solving a very practical problem: to model forces and frictions inducing the complicated oscillations he observed and to predict behaviors in general. His results are contained in an interesting and readable monograph [5] in which the work done in the field by his predecessors is reviewed critically, including works by Braun (1874) and Rayleigh (1894). Duffing discusses in detail analytical and numerical approximations to the solutions of the generic differential equation

$$\ddot{x} + a\dot{x} + \alpha x + \beta x^2 + x^3 = b \cdot f(t), \quad (1)$$

where $f(t)$ is a periodic function driving the system. Further, he presents exact analytical solutions not only for the $b = 0$ “no-drive” limit (in terms of elliptic functions as defined by Weierstrass) but considers also several limits with $b \neq 0$, presenting in particular approximate solutions for situations in which Eq. (1) has one and/or two potential wells driven periodically by a trigonometric function. Here we refer to “Duffing equation” as being the particular single-well equation

$$\ddot{x} + a\dot{x} + x^3 = b \cdot f(t), \quad (2)$$

where x and t are the dependent and independent variables, respectively, and a and b are adjustable parameters of the model. We concentrate on this one-well form of the equation because there is already an immense body of results for it. In particular, when driven with $f(t) = \cos(t)$, Eq. (2) was considered previously by Hayashi [6] and Ueda [7] among other researchers. Holmes [8] studied another of the equations considered by Duffing.

Hayashi presents a remarkably detailed investigation of periodic motions, giving impressive figures dis-

playing results obtained not only from numerical studies, but also from analytical approximations of the invariant manifolds of periodic orbits. He presents *analytic* approximations of the “separatrix” curves [i.e. of *basin boundaries* in different parlance] and describes *quantitatively* how these curves emanate from saddle points on the boundary and how they organize themselves in phase space. Ueda, in pioneering contributions published since 1961 [9], realized the existence and the importance of aperiodic motions. Among many other things, he reported [7] aperiodic behaviors for $a = 0.1$ and for six points b in the interval $10.0 < b < 13.3$ and for $b = 12$ and for nine points in the interval $0.01 \leq a \leq 0.34$. A detailed account of the contributions from the “Kyoto school” to the understanding of driven oscillators and to the “birth of chaos” is given by Ueda [9] in a fascinating book which also contains English translations of papers published originally in Japanese.

The present paper reports results of two numerical experiments based on Eq. (2). First, driving Eq. (2) with $f(t) = \cos(t)$ we compute a diagram in the space $a \times b$ of Eq. (2) showing parameter regions where one finds periodic behaviors and where there is aperiodic (“chaotic”) behavior. From this result (shown below in Fig. 7) one recognizes that there is a surprising relatively self-similar repetition of islands characterized by positive exponents (i.e. aperiodic behaviors) embedded in seas of negative exponents (periodic behaviors). We believe Fig. 7 below to be the first one to provide a detailed view of the dichotomous division over an extended region of the parameter space for a *continuous-time* dynamical system. In contrast with the situation familiarly observed in parameter space of *discrete-time* dynamical systems (i.e. discrete mappings), where one frequently finds islands of periodicity embedded in chaotic “phases” [10,11], in the parameter space of the continuous-time Duffing oscillator this paper reports the opposite: islands of chaos embedded in wide seas of regularity (periodicity).

In the second numerical experiment, with results shown in Figs. 10 and 11 below, we study what happens with the “islands of chaos” when one changes externally the nature of the periodic driving force. An easy and convenient way of driving the system with

a periodic force having a more sophisticated Fourier spectrum than a $\cos(t)$ is to drive it with a Jacobian elliptic function, a quite natural choice since Jacobian functions are exact analytical solutions of the differential equation in the absence of forcing [5,12,13]. Specifically, we consider quantitatively what happens to Eq. (2) when driven with the Jacobian elliptic function

$$f(t) = \text{cn}(t, m). \quad (3)$$

By varying the parameter m one may conveniently and continuously move from the standard trigonometric pumping for $m = 0$, when $\text{cn}(t, 0) \equiv \cos(t)$, to a hyperbolic pumping for $m = 1$, when $\text{cn}(t, 1) \equiv \text{sech}(t)$. For m -values in the range $0 < m < 1$ one has intermediary pumpings with rich and regular Fourier spectra (see Fig. 4 below.)

An interesting finding while driving the system externally with more general periodic functions is that it is possible to clean regions in parameter space from chaotic behavior by displacing the chaotic islands. Cleaning parameter regions from chaos by tuning external drives may be of interest in experimental situations where model parameters are more difficult to change (or when one does not want to change them) than those of the drive. Lasers systems with modulation either in the losses of the resonator, in the pump or in the resonator frequency are natural examples of systems that could be cleaned from chaos by suitably tuning external drives. For a recent review on instabilities in lasers see Ref. [14].

In one form or another, Duffing equations have already been considered by several workers. For recent references see, for example, Refs. [8,15–28] and the references therein. In recent years the emphasis has been in studying “chaotic” behaviors, i.e. recurrent aperiodic motions, which appear when exciting the system. In this context, we mention an interesting possibility of suppressing chaos in the Duffing oscillator by resonant parametric perturbations as recently discussed both theoretically and experimentally [29]. Among other things, some works have concentrated on the investigation of the structure of basin boundaries for the more general case of the Duffing equation, also in situations having two wells [9,15].

The paper is organized as follows. In the next section, Section 2, we consider some practical aspects of the computation of Lyapunov exponents. In Section 3, we review briefly some well-known properties of elliptic functions that are of interest in the present context. In Section 4, we present results for the case of trigonometric pumping. In Section 5 we present results obtained for $m > 0$, closing in Section 6 with some general conclusions about forced oscillations induced by Jacobian elliptic functions. For completeness, we mention that some aspects of elliptic functions acting as discrete dynamical systems were already considered in earlier work [13,30].

2. Numerical details

The study of continuous-time dynamical systems requires the repeated numerical integration of systems of differential equations. A number of commonly used numerical methods of integration and their performances have been recently contrasted in an interesting paper by Cartwright and Piro [31], which also contains additional references. In the present work we integrate Eq. (2) with a fourth-order Runge–Kutta integrator with fixed step size h , a standard choice which we also find to provide a good compromise between speed and accuracy.

There are three easily discernible time scales involved in the numerical solution of ordinary differential equations similar to Eq. (2): a *microscopic* time scale defined by the time step h used to advance the numerical solution, a *macroscopic* time scale determined by the total number \mathcal{N} of time steps h spent observing the system, and an *intermediate* time scale dictated by the period P of the driving force. For a given fixed value of P one needs to find “reasonable” working values for h and \mathcal{N} in order to be able to perform reliable numerical experiments. The compromise sought for is familiar: to find numerical values for h small enough to guarantee the reliability of the numerical algorithms used but simultaneously large enough to allow following the dynamics during time intervals such that one might feel confident of being “sufficiently” close to asymptotic regimes of interest

and then follow the dynamics during reasonable intervals of time. The period P is the standard time scale used to define Poincaré sections when observing the system stroboscopically.

The method of determining Lyapunov exponents is based on the investigation of the growth of vectors tangent to the surface defined by the equations of motion in the phase space of the physical system. The formalism to compute Lyapunov exponents that one finds in the literature [1–4] assumes the equations of motion to be time independent. Therefore, to use this formalism one needs to write Eq. (2) with the forcing defined by Eq. (3) as an autonomous system, obtaining the set

$$\dot{x}_1 = x_2, \quad (4)$$

$$\dot{x}_2 = -ax_2 - x_1^3 + b \operatorname{cn}(x_3, m), \quad (5)$$

$$\dot{x}_3 = 1.0, \quad (6)$$

$$\dot{\xi}_1 = \xi_2, \quad (7)$$

$$\dot{\xi}_2 = -3x_1^2\xi_1 - a\xi_2 - b\xi_3 \operatorname{sn}(x_3, m), \quad (8)$$

$$\dot{\xi}_3 = 0.0, \quad (9)$$

where the three last equations are the *variational equations* [32] corresponding to the first three ones, which are equivalent to Eq. (2). The $\dot{\xi}_i$ define the tangent space from which one obtains characteristic Lyapunov exponents by studying the time evolution of volumes [2,3].

All exponents reported in this paper are obtained as follows. We integrate Eqs. (4)–(9) fixing arbitrarily $\xi_1(0) = \xi_2(0) = 1.0$ and $\xi_3(0) \equiv t_0 = 0.0$ as the initial conditions for the variational system. As is known, for some classes of dynamical systems Oseledec [1] has shown that, with the possible exception of a set of measure zero, exponents are independent of the initial conditions of the variational equations. Unfortunately there seems to exist no simple way to guarantee this independence for many models of interest, in particular for the one under investigation here. When nothing else is said, the following arbitrary initial conditions were used for the three variables: $x_1(0) = 0.0$, $x_2(0) = -6.0$ and $x_3(0) = 0.0$. Starting from these initial conditions we integrated Eqs. (4)–(9) during a certain number of cycles of the drive (the “transient”

time, almost always 200 cycles, the only exceptions being indicated in Figs. 1, 5 and 6 below), so that the system would be close enough to the final attractor. After that, we started the computation of Lyapunov exponents during another number of cycles, a number never smaller than the aforementioned transient time.

We consider now the dependence of Lyapunov exponents on the time step h used in the Runge–Kutta integration of Eqs. (4)–(9). To this end Eqs. (4)–(9) are integrated for two sets of parameters motivated by previous work of Ueda [7]: $(a, b) = (0.1, 13.5)$ and $(0.1, 13.3)$. Asymptotically, the first set produces periodic motion while the second produces an aperiodic (“chaotic”) motion. We assume the driving force to be $\cos(t)$, and compare exponents obtained by discretizing one period $P = 2\pi$ using 12 different values $h_i = 2\pi/k_i$, namely, $h_i \simeq 0.2513, 0.2094, 0.1256, 0.0837, 0.0628, 0.0200, 0.0125, 0.0100, 0.0062, 0.0041, 0.0031, 0.0020$, respectively for $k_i = 25, 30, 50, 75, 100, 314, 500, 628, 1000, 1500, 2000$ and 3000.

Fig. 1 shows exponents calculated by integrating Eqs. (4)–(9) during four different intervals M/N of time: 100/50, 200/100, 400/100 and 400/200, where M gives the total number of cycles of $\cos(t)$ during which exponents were calculated, *after* disregarding N preliminary cycles as being a transient time needed to come sufficiently close to the asymptotic attractor associated with the initial conditions. The total integration time is $N + M$ cycles. From Fig. 1 one sees that $h < 0.1$ seems to be already a step size small enough to produce converged exponents, even for the aperiodic trajectory. Further, Fig. 1 indicates that after a transient of 200 cycles the system is already close enough to the asymptotic trajectory. The figure also shows that as h decreases, residual fluctuations of the exponents are significantly smaller in the case of the periodic attractor. The behavior displayed by these two orbits is qualitatively similar to the behavior observed for a few other arbitrarily chosen parameters and initial conditions. Based on the results in Fig. 1 we fixed $h = 0.02$ in all subsequent computations for $m = 0$. Notice that h is the quantity defining the price to be paid to obtain each exponent, namely the total number of steps that one needs to integrate the differential

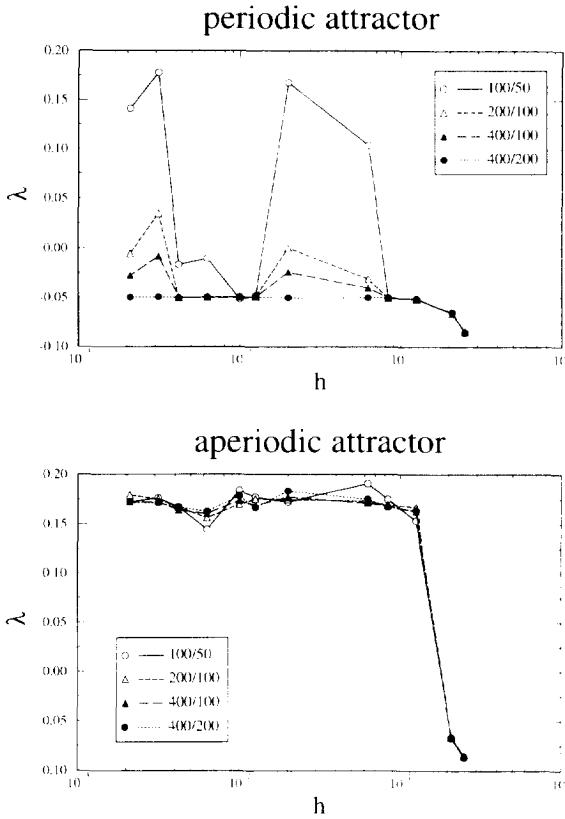


Fig. 1. Dependence of Lyapunov exponents on the step h of integration, on the interval of integration and on the time needed to reach the attractor; 100/50 means that exponents were calculated during 100 cycles of the drive after disregarding 50 cycles as transients, etc. The periodic attractor is for $(a, b) = (0.1, 13.5)$; the aperiodic one, for $(0.1, 13.3)$. Here $m = 0$.

equations: while one needs only 10^4 time steps to obtain the data presented in Fig. 1 for 400 cycles of the drive with $h = 0.2513$, roughly 120×10^4 time steps are need to cover the same 400 cycles when using $h = 0.0020$.

The period of the drive depends on m as shown in Fig. 2. For $m \neq 0$ we also used $h = 0.02$, obviously requiring increasingly more time steps to cover one period of the drive as m increases. We noticed that frequently the step size $h = 0.02$ and the number of cycles for integrations could be significantly decreased without producing visually noticeable changes in final diagrams (as in Fig. 6 below, for example.) However, in the absence of more detailed investigations about the effects of these two parameters, we preferred to

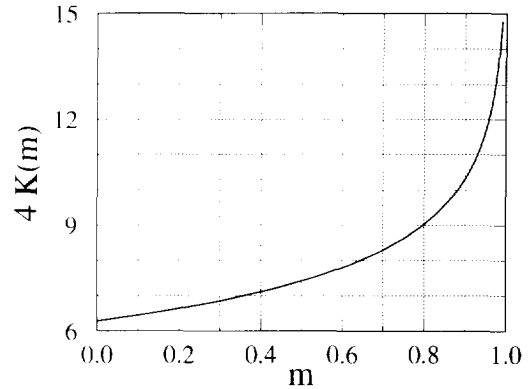


Fig. 2. Period of the Jacobian elliptic $\text{cn}(t, m)$ as function of m . For $m = 0.99$ one has $4K(m) \simeq 14.782549$. For $m = 1$ the period is asymptotic to ∞ .

maintain the more stringent bounds for the time being.

Almost all exponents reported in this paper were computed using up to 140 nodes in parallel, “farming”, on an Intel Paragon XP/S 10, a scalable distributed multicomputer. Each of these nodes contains two i860 XP microprocessors (application processor, message processor), whose clock speed is 50 MHz, and 32 MB of memory. The theoretical peak performance of the i860 XP is 75 MFLOPS (64-bit arithmetic). In other terms, sets of exponents were computed in parallel by an array of up to 140 workstations, each one computing a slice either in parameter or phase space. The average time required to compute a single exponent for $m = 0$ (i.e. without having to evaluate elliptic functions) is of the order of 7.5 seconds for integrations with $h = 0.02$ over 400 cycles of the drive. For $m \simeq 0.5$ the average time is about 54.8 seconds per exponent while for $m \simeq 0.999$ it takes about 64.3 seconds per exponent, all computations done in double precision.

3. Jacobian elliptic functions

We now review briefly some well-known properties of Jacobian elliptic functions that are necessary to understand the nature of the driving force with which we want to force the Duffing oscillator. As mentioned above, it is possible to solve analytically

Eq. (2) [as well as generalizations of it containing linear and quadratic terms as in Eq. (1)] when there is no forcing and no friction acting in the system. For solutions in terms of the elliptic functions of Weierstrass see Duffing [5] or Reynolds [12]. For solutions in terms of Jacobian elliptic functions see Ref. [13]. Further, according to Ref. [33], it should be possible to find analytical solutions for some particular cases of slightly more general Duffing equations in which although there is no forcing, there is friction acting on the system. All these solutions are in terms of elliptic functions. Basic facts about elliptic functions and integrals may be found, for example, in the articles by Milne-Thomson [34].

Altogether there are twelve Jacobian elliptic functions, all doubly-periodic meromorphic functions. They have a real and an imaginary period depending on a parameter m bounded to the interval $0 \leq m \leq 1$. Of particular interest are the elliptic functions $\text{cn}(t, m)$ and $\text{sn}(t, m)$, which for $m = 0$ reduce themselves to the familiar $\cos(t)$ and $\sin(t)$ functions, respectively. The real period of these elliptic functions is given by

$$P = 4K(m), \tag{10}$$

where $K(m)$ is the elliptic integral

$$K(m) \equiv K = \int_0^{\pi/2} \frac{d\theta}{[1 - m \cdot \sin(\theta)]^{1/2}}. \tag{11}$$

For $m = 0$ one has $K(0) = \pi/2$. Fig. 2 shows the period $4K(m)$ for other not so trivial values of m .

The function $\text{cn}(t, m)$ which will be used to drive Duffing's oscillator may be expressed as an infinite series expansion in terms of the nome $q = e^{-\pi K'/K}$ and the argument $v = \pi u/(2K)$ as follows (Ref. [34], p. 575, Eq. 16.23.2):

$$\text{cn}(u, m) = \frac{2\pi}{m^{1/2}K} \sum_{n=0}^{\infty} \frac{q^{n+1/2}}{1 + q^{2n+1}} \cos[(2n + 1)v], \tag{12}$$

where K' (which appears in the nome q) is defined by

$$K'(m) \equiv K' = \int_0^{\pi/2} \frac{d\theta}{[1 - (1 - m) \cdot \sin(\theta)]^{1/2}}. \tag{13}$$

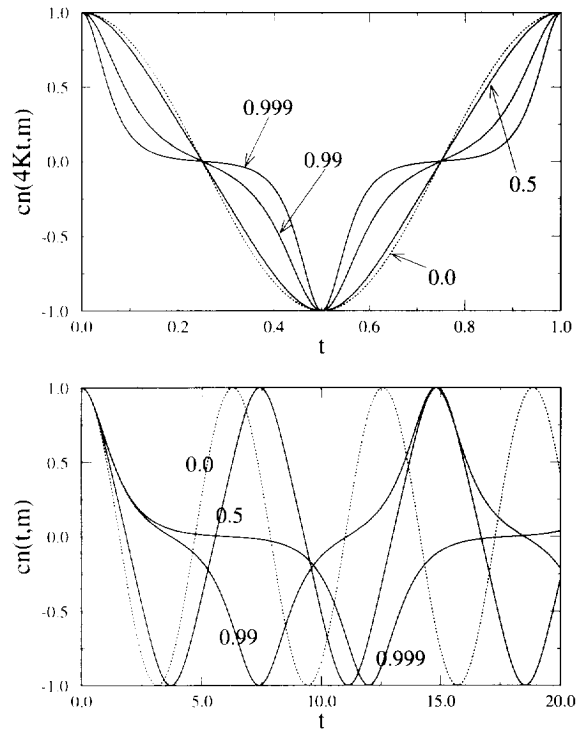


Fig. 3. Modifications of the waveform and periodicity of the elliptic function $\text{cn}(t, m)$ for some values of m , as indicated by the numbers. Dotted lines correspond to $\cos(t)$. By varying m one changes simultaneously the waveform and the period of the drive.

$K(m)$ was efficiently and accurately computed with the algorithm R_f given by Carlson [35]. The $\text{cn}(t, m)$ function was computed using the arithmetic-geometric mean algorithm described by Milne-Thomson [34].

Fig. 3 presents graphs of $\text{cn}(t, m)$ for some values of m . One clearly sees the changes introduced by the parameter m , both in the waveform of the oscillation and in its period. To better understand the Jacobian driving function and in addition to the analytical expression above, Fig. 4 shows Fourier transforms (taken as the square-root of the sum of the square of the spectral amplitudes) obtained numerically from time series containing 20 cycles of $\text{cn}(t, m)$.

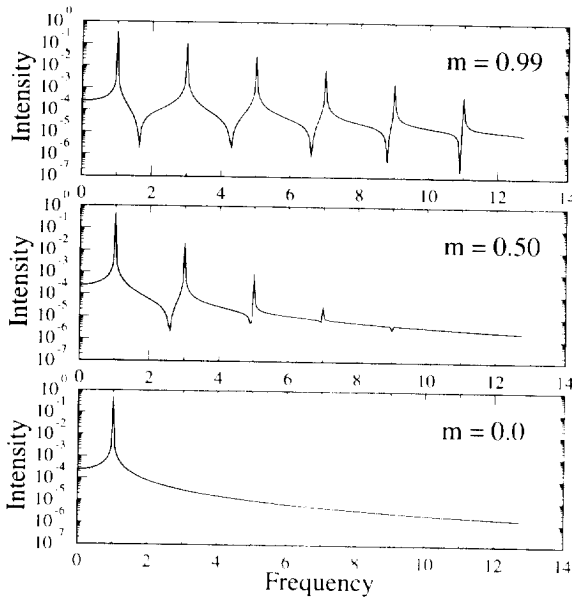


Fig. 4. Fourier spectrum of the function $cn(t, m)$ for three values of m , as indicated. For $m = 0$ one has $cn(t, 0) \equiv \cos(t)$.

4. Results for $m = 0$: Effects of trigonometric driving

In this section we reconsider the behavior of Duffing's equation when driven with the trigonometric pumping $f(t) = \cos(t)$. We start by studying first two slices of the parameter space containing the points originally investigated by Ueda [7] and, more recently, by Moon [15].

Fig. 5 illustrates the behavior of the exponents for the slice of the parameter space defined at $a = 0.1$. Superimposed in Fig. 5 one sees the six numerical values reported by Ueda. The agreement of both sets of exponents is quite good. Further one clearly sees that the b values studied by Ueda define a quite characteristic "window" of aperiodic motion along the $a = 0.1$ slice. Ueda considered also the slice defined at $b = 12.0$ for $0.01 \leq a \leq 0.34$. Our values for this case are shown in Fig. 6, again with the values of Ueda superimposed. The agreement is once more quite good. A distinctive feature of both cuts is that while for constant dissipation the minimum value of the exponents remains constant, exponents decrease in general when the dissipation increases while maintaining fixed the

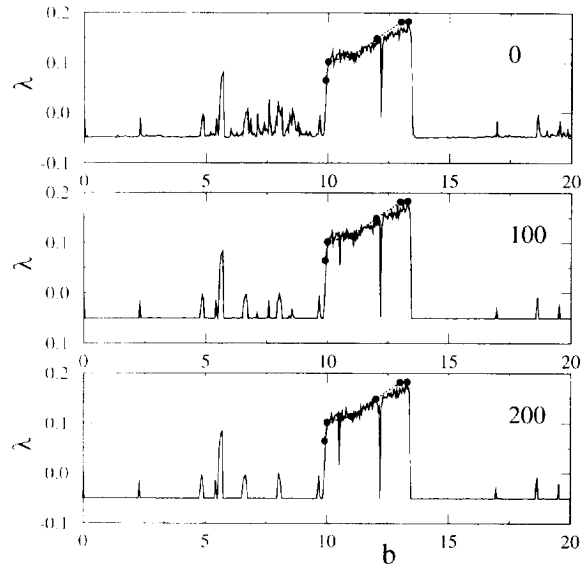


Fig. 5. The $a = 0.1$ slice of the window of aperiodic behavior discovered by Ueda [7]. Shown are 500 exponents, each one calculated during 400 cycles of the drive which follow after transients of 0, 100 and 200 cycles, as indicated, from initial conditions defined in Section 2. The six dots are values from Ueda.

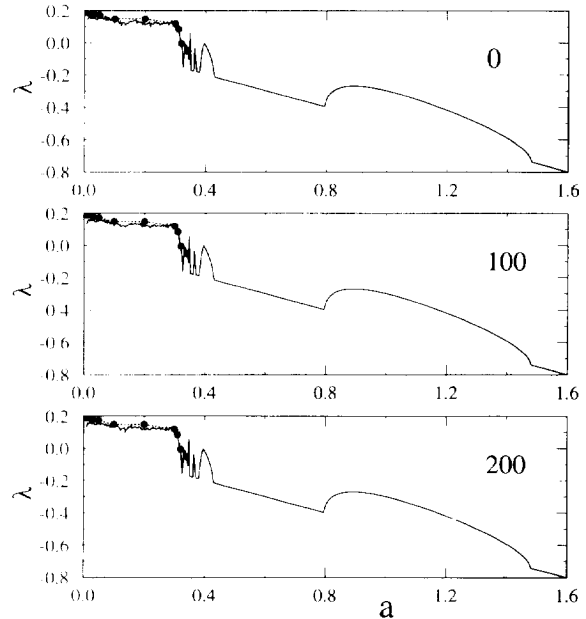


Fig. 6. The $b = 12.0$ slice of the window of aperiodic behavior discovered by Ueda [7]. Shown are 500 exponents, each one calculated during 400 cycles of the drive which follow after transients of 0, 100 and 200 cycles, as indicated, from initial conditions defined in Section 2. The nine dots are values from Ueda.

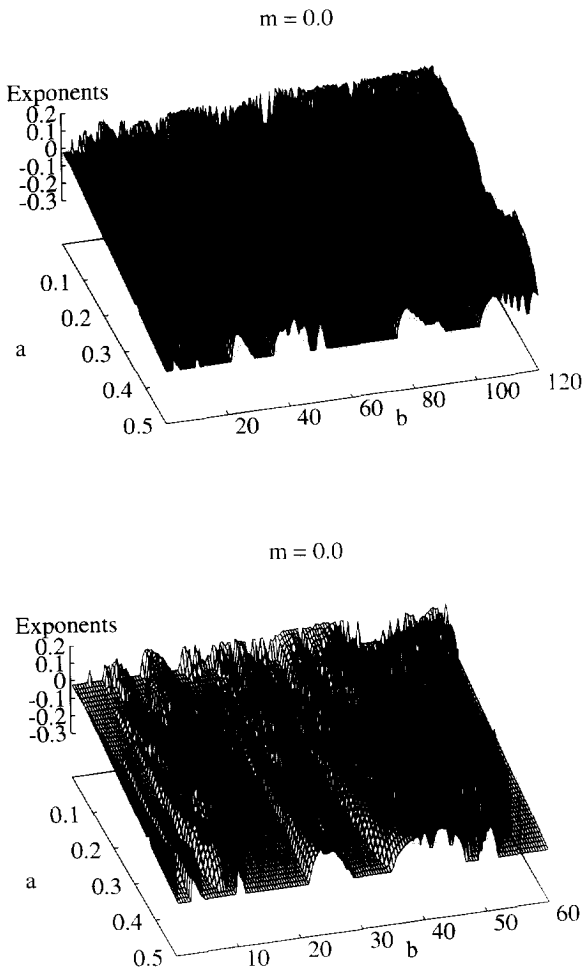


Fig. 7. Exponents as obtained under trigonometric pumping. The lower view is a magnification of the first half of the view on the top.

oscillation amplitude.

Fig. 7 shows 50×300 exponents for a relatively extended region in parameter space: $0.0 \leq a \leq 0.5$, discretized into 50 equally spaced intervals, and $0 \leq b \leq 120$, discretized into 300 equal intervals. Individual slices of the surface shown in this figure having either a or b constant are qualitatively similar to the slices shown in Figs. 5 and 6. As seen from Fig. 7, exponents appear as sequences of “mountains” parallel to the a axis, made by more or less concentric nestings of parabolic components.

A recent study [10,11] provided detailed parameter-space diagrams for discrete-time dynamical systems

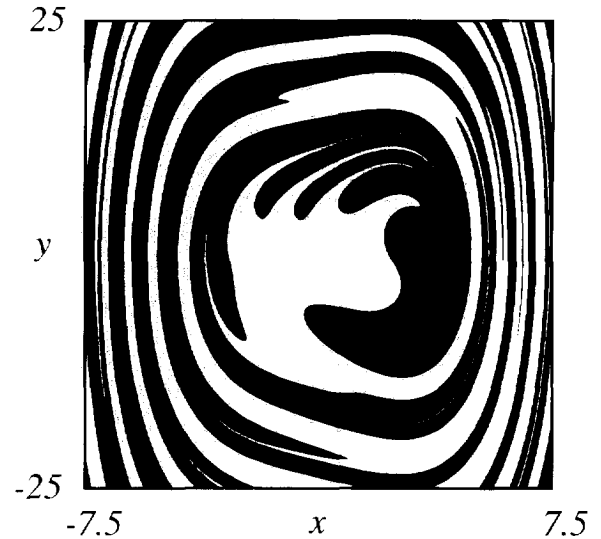


Fig. 8. Basins of attraction for periodic motions (white shading) and aperiodic motions (black shading). The figure is a PostScript bitmap containing 900×900 exponents for $(a, b) = (0.1, 13.3)$. Here $x \equiv x_1$ and $y \equiv x_2$, with x_i as in Eqs. (4) and (5). Basins for other parameter values are given by Ueda in Ref. [9] and in other references quoted therein.

showing the location of a “Via Caotica” [10], i.e. regions of parameters characterized by supporting aperiodic motions with relatively large basins of attraction. Embedded in these regions of chaotic parameters one finds a number of easily discernible “directions” along which *windows of periodicity* appear in a quite organized way. Such windows appear frequently as characteristic self-similar shapes, a typical example being the “shrimps” discussed in Refs. [10,11]. Knowing the existence of such regularities in the parameter space of discrete-time dynamical systems, it is natural to ask whether similar structures might be present in the parameter space of continuous-time dynamical systems. For continuous-time dynamical systems the explicit characterization of periodicities for each individual pair (a, b) although in principle elementary, requires additional computer time. From Fig. 7 one sees that in the present continuous-time dynamical system there are *parameter domains characterized by chaotic behaviors arising systematically aligned in a quite regular fashion*. It is important to call attention to the fact that all figures in this paper are obtained without approximations. They have their

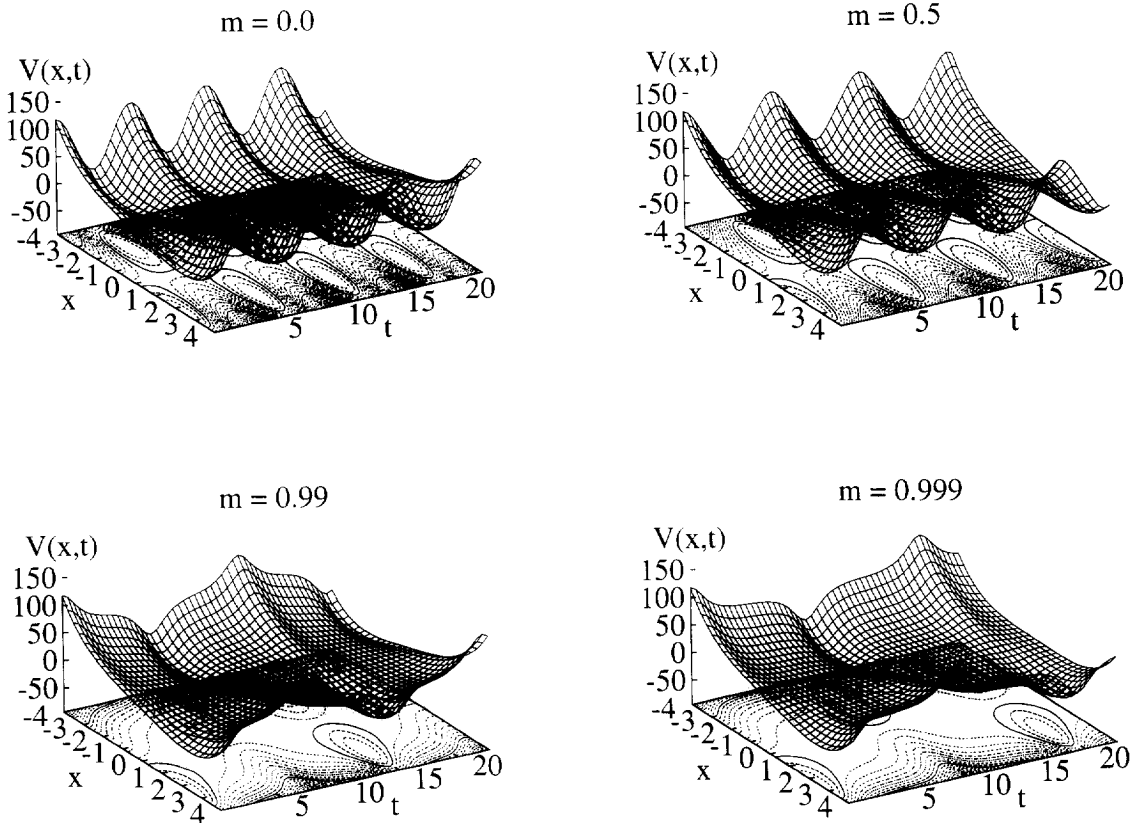


Fig. 9. Duffing's potential: $V(x,t) = \frac{1}{4}x^4 - x \cdot b \cdot cn(t,m)$, here for $b = 0.05$.

accuracy determined only by the high intrinsic accuracy with which one generates numerical solutions of ordinary differential equations. The question concerning the variation of periodicities in regions between (or inside) different "islands" of chaotic parameters requires spending additional computer time. We plan to consider this interesting question in subsequent work.

Fig. 8 shows examples of basins of attraction, here determined for periodic (white shading) and chaotic (black shading) attractors coexisting for $a = 0.1$ and $b = 13.3$. It is important to notice that the basins in Fig. 8 were determined by calculating Lyapunov exponents, not by following the time evolution of the solution and recording those that enter (or not) a ball around a fixed point. Basins of attraction similar to those in Fig. 8 were found for many other parameter values. An important open problem requiring exten-

sive computations is the determination of the extension and structure of non-measure-zero basins of attraction for *all* possible attractors associated with fixed sets of parameters.

5. Results for $m \neq 0$: Effects of Jacobian driving

We now consider changes induced in the shape and location of islands of aperiodic solutions when driving the system with $f(t) = cn(t,m)$ and varying m . In this case the potential function acting on Duffing's equation is defined by

$$V(x,t) = \frac{1}{4}x^4 - x \cdot b \cdot cn(t,m). \tag{14}$$

This potential is shown for four values of m in Fig. 9. From this figure one sees that as m increases, the overall physical effect of the elliptic function is to intro-

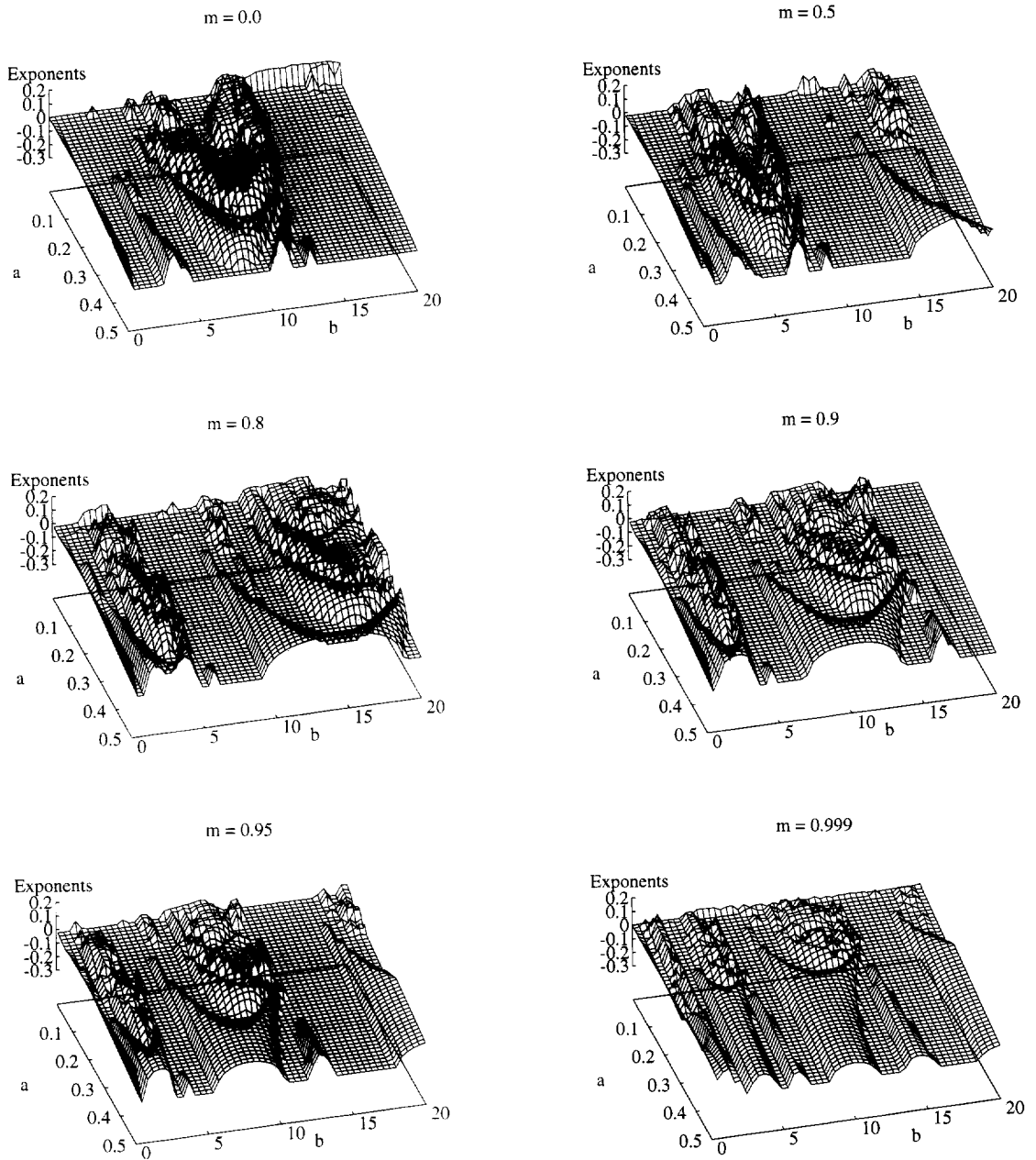


Fig. 10. Evolution of the island of aperiodic behavior. Each picture shows 50×50 exponents calculated during 400 cycles of the drive following a transient of 200 cycles.

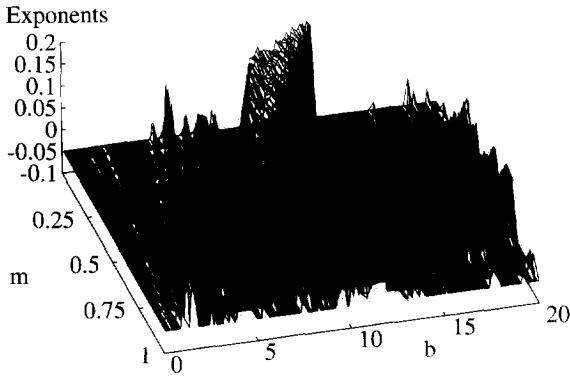


Fig. 11. Dependence of the exponents on m , on a $m \times b = 20 \times 250$ mesh. The maximum value of m plotted is $m = 0.999$. In this figure, $a = 0.1$ and initial conditions as defined in Section 2.

duce wide regions along which the potential varies less and less in time, compared with what happens near the peaks and valleys which are characterized by having their amplitudes independent of m and having relatively abrupt and localized variations.

Fig. 10 shows the changes in the $a \times b$ space as m increases from 0 to 0.999. From this figure one easily recognizes that the effect of increasing m is to introduce a “double-compression” in the system: all islands are pushed towards the line $b = 0$, being simultaneously compressed towards the line $a = 0$. This implies that as m increases the density of parameters characterized by aperiodic motions increases along lines of constant b (amplitude of the driving force) and decreases along lines of constant a (strength of the dissipation).

Fig. 11 shows the evolution of the exponents when we fix the strength of the dissipation at $a = 0.1$ and increase m . Shown are 15×250 exponents for 250 equally spaced values of b in the interval $0 \leq b \leq 20$ and 15 equally spaced values of m covering the interval $0.0 \leq m \leq 0.999$. One sees a strong increase of the density of parameters supporting aperiodic solutions as m increases. Further, one sees that there are “valleys” between the “mountains” (which signal parameters leading to aperiodic solutions) and that these valleys become quite narrow as m increases.

6. Conclusions

This paper reported a systematic investigation of the parameter space of the single-well Duffing oscillator defined in Eq. (2) with $f(t) = cn(t, m)$. We used Lyapunov exponents to perform a dichotomous division of the parameter space into (i) regions characterized by parameters for which one finds quite large basins of attraction for *aperiodic solutions* (positive exponents), and (ii) regions characterized by *periodic solutions* (non-positive exponents). When driven by a $\cos(t)$ function, the parameter space of the Duffing equation contains a series of parallel “islands” of parameters characterized by aperiodic attractors with wide basins of attraction as shown in Fig. 7. The aperiodic solutions discovered originally by Ueda are located in the first such island. Many other similar islands are observed when increasing the amplitude of the driving force. In addition, we find that it is possible to displace the island corresponding to aperiodic behaviors as shown in Fig. 10 by using $cn(t, m)$ instead of $\cos(t)$ [$\equiv cn(t, m = 0)$] as the driving force and tuning the parameter m . This externally induced displacement effect may be conveniently exploited in experiments, for example, to “clean” regions of parameters from chaotic behaviors or to bring chaotic motions to parameter locations of interest. The possibility of altering the periodicity of solutions over extended regions of parameters via external periodic pumping might be helpful in experimental situations where changes in other “internal” parameters may not be as easy to accomplish.

As m increases one observes a clear increase in the density of parameters corresponding to aperiodic solutions, meaning that chaotic behaviors are much more likely to be found in this case. An interesting open question is the investigation of the “fine-structure” of both periodic and aperiodic domains of parameters, determining, for example, their “degeneracies”, namely, the number of different attractors in each domain and classifying the variation of periodicities for solutions corresponding to non-positive exponents. We hope to be able to report some of these results soon.

Acknowledgements

J.G. thanks Julyan Cartwright and Oreste Piro for informative discussions at “The Gran Finale” Conference, Como, Italy. He thanks Prof. W. Lauterborn for kindly providing reprints of Refs. [22,23] and Prof. C. Grebogi for his kind interest in our work and for calling attention to Ref. [18]. J.G. is also very much indebted to Prof. Y. Ueda for bringing Ref. [9] to his attention and for helpful correspondence, and to Prof. B.C. Carlson for providing (in 1980) the original routines used to compute elliptic functions and integrals here.

References

- [1] V.V. Nemytskii and V.V. Stepanov, *Qualitative theory of differential equations* (Princeton Univ. Press, Princeton, 1960);
V.I. Oseledec, *Trans. Moscow Math. Soc.* 19 (1968) 197;
J.B. Pesin, *Russ. Math. Surv.* 32 (1977) 55.
- [2] G. Benettin, L. Galgani and J.M. Strelcyn, *Phys. Rev. A* 14 (1976) 2338;
G. Benettin, L. Galgani, A. Giorgilli and J.M. Strelcyn, *Meccanica* 15 (1980) 9–20, 21–30.
- [3] I. Shimada and T. Nagashima, *Prog. Theor. Phys.* 61 (1979) 1605.
- [4] A. Wolf, J.B. Swift, H.L. Swinney and J.A. Vastano, *Physica D* 16 (1985) 285;
J.-P. Eckmann and D. Ruelle, *Rev. Mod. Phys.* 57 (1985) 617;
M. Sano and Y. Sawada, *Phys. Rev. Lett.* 55 (1985) 1082.
- [5] G. Duffing, *Erzwungene Schwingungen bei veränderlicher Eigenfrequenz und ihre technische Bedeutung*, Sammlung Vieweg, Heft 41/42 (Braunschweig, 1918).
- [6] C. Hayashi, *J. Appl. Phys.* 24 (1953) 198, 344, 521;
C. Hayashi, *Nonlinear oscillations in physical systems* (McGraw-Hill, New York, 1964); *Int. J. Non-Linear Mech.* 15 (1980) 341.
- [7] Y. Ueda, *J. Stat. Phys.*, 20 (1979) 181; *Ann. N.Y. Acad. Sci.* 357 (1980) 422; *Steady motions exhibited by Duffing’s equation: A picture book of regular and chaotic motion*, in: *New Approaches to Non-linear Problems in Dynamics*, P.J. Holmes, ed. (SIAM, Philadelphia, 1980); *the review in Chaos, Solitons Fractals* 1 (1991) 199.
- [8] P. Holmes, *Phil. Trans. R. Soc. A* 292 (1979) 419;
P. Holmes and D. Whitley, *Physica D* 7 (1983) 111;
J. Guckenheimer and P. Holmes, *Nonlinear Oscillations, Dynamical Systems, and Bifurcations of Vector Fields*, 3rd Ed. (Springer, New York, 1990).
- [9] Y. Ueda, *The Road to Chaos* (Aerial Press Inc., P.O. Box 1360, Santa Cruz, CA 95061, USA, ISBN 0-942344-14-6, 1992).
- [10] J.A.C. Gallas, *Phys. Rev. Lett.* 70 (1993) 2714.
- [11] J.A.C. Gallas, *Appl. Phys. B* 60 (1995) S-203; *Physica A* 211 (1994) 57; 202 (1994) 196.
- [12] M.J. Reynolds, *J. Phys. A* 22 (1989) L723.
- [13] J.A.C. Gallas, *Int. J. Bif. Chaos* 3 (1993) 451.
- [14] C.O. Weiss and R. Vilaseca, *Dynamics of Lasers* (VCH, Weinheim, 1991).
- [15] F.C. Moon and G.-X. Li, *Phys. Rev. Lett.* 55 (1985) 1439;
F.C. Moon, *Chaotic and Fractal Dynamics* (Wiley, New York, 1992).
- [16] Y. Ueda, S. Yoshida, H.B. Stewart and J.M.T. Thompson, *Phil. Trans. R. Soc. London A* 332 (1990) 169.
- [17] J. Miles, *Proc. Natl. Acad. Sci.* 81 (1984) 3919; *Physica D* 31 (1988) 252; *Phys. Lett. A* 130 (1988) 276.
- [18] A.N. Lansbury, J.M.T. Thompson and H.B. Stewart, *Int. J. Bif. Chaos* 2 (1992) 505.
- [19] G. Eilenberger and K. Schmidt, *J. Phys. A* 25 (1992) 6335.
- [20] A. Belogortsev, *Nonlinearity* 5 (1992) 889.
- [21] C.S. Wang, Y.H. Kao, J.C. Huang and Y.S. Gou, *Phys. Rev. A* 45 (1992) 3471.
- [22] U. Parlitz and W. Lauterborn, *Phys. Lett. A* 107 (1985) 351; *Phys. Rev. A* 36 (1987) 1428;
U. Parlitz, *Int. J. Bif. Chaos* 3 (1993) 703.
- [23] V. Englisch and W. Lauterborn, *Phys. Rev. A* 44 (1991) 916;
C. Scheffczyk, U. Parlitz, T. Kurz, W. Knop and W. Lauterborn, *Phys. Rev. A* 43 (1991) 6495;
R. Mettin, U. Parlitz and W. Lauterborn, *Int. J. Bif. Chaos* 3 (1993) 1529.
- [24] T.L. Carroll and L.M. Pecora, *Phys. Rev. E* 43 (1993) 3941.
- [25] B. Mehri and M. Ghorashi, *J. Sound Vibr.* 169 (1994) 289.
- [26] L.N. Virgin and K.D. Murphy, *J. Sound Vibr.* 169 (1994) 699.
- [27] A.F. Vakakis, *J. Sound Vibr.* 170 (1994) 119.
- [28] B. Ravindra and A.K. Malik, *Phys. Rev. E* 49 (1994) 4950.
- [29] R. Lima and M. Petini, *Phys. Rev. A* 41 (1990) 726;
L. Fronzoni, M. Giocondo and M. Petini, *Phys. Rev. A* 43 (1991) 6483;
F. Cuadros and R. Chancon, *Phys. Rev. E* 47 (1993) 4628;
R. Lima and M. Petini, *Phys. Rev. E* 47 (1993) 4630.
- [30] J.A.C. Gallas, *Int. J. Mod. Physics C: Physics and Computers* 3 (1992) 553.
- [31] J.H.E. Cartwright and O. Piro, *Int. J. Bif. Chaos* 2 (1992) 427.
- [32] H. Poincaré, *Acta Math.* 13 (1890) 3–271.
- [33] N. Euler, W.-H. Steeb and K. Cyrus, *J. Phys. A* 22 (1989) L195.
- [34] L.M. Milne-Thomson, in: *Handbook of Mathematical Functions*, M. Abramowitz and I. Stegun, eds. (Dover, New York, 1965), articles on pp. 567 and 582.
- [35] B.C. Carlson, *Num. Math.* 33 (1979) 1.